IOP Publishing | Royal Swedish Academy of Sciences Physica Scripta
Phys. Scr. **89** (2014) 044002 (5pp) doi:10.1088/0031-8949/89/04/044002

Local structure studies of $SrTi^{16}O_3$ and $SrTi^{18}O_3$

A Anspoks[1], D Bocharov[1], J Purans[1], F Rocca[2], A Sarakovskis[1], V Trepakov[3,4], A Dejneka[4] and M Itoh[5]

[1] Institute of Solid State Physics, University of Latvia, Riga LV-1063, Latvia
[2] IFN-CNR, Institute for Photonics and Nanotechnologies, Unit FBK-Photonics of Trento, Povo, Trento, Italy
[3] Ioffe Physical-Technical Institute RAS, Saint-Petersburg, Russia
[4] Institute of Physics, AS CR, Prague, Czech Republic
[5] Tokyo Institute of Technology, Tokyo, Japan

E-mail: andris.anspoks@cfi.lu.lv

Received 6 June 2013, revised 26 July 2013
Accepted for publication 30 July 2013
Published 25 February 2014

Abstract

In this work we report on the local structure of Ti in $SrTi^{16}O_3$ (STO16) and $SrTi^{18}O_3$ (STO18) investigated in the low temperature range (6–300 K) by extended x-ray absorption fine structure and x-ray absorption near edge structure (XANES) spectroscopy at Ti K-edge and by optical second harmonic generation (SHG). By comparing XANES of STO16 and STO18 we have identified the isotopic effect which produces at $T < 100$ K a noticeable difference in the measured mean square relative displacements (MSRD) of Ti–O_1 bonds: while STO16 follow the expected Einstein-like behavior, for STO18 we have measured an increase of MSRD values with decreasing temperature. This is an indication of an increasing off-center position of the Ti atoms in the TiO_6 octahedra.

PACS numbers: 61.05.cj, 78.70.Dm, 77.80.B−, 42.65.Ky

(Some figures may appear in colour only in the online journal)

1. Introduction

Strontium titanate ($SrTiO_3$) (STO) is a very popular and thoroughly studied compound that is representative of the family of ABO_3 oxides and related materials [1]. At room temperature (RT) it adopts the cubic O_h^1 perovskite-type structure. At $T_f = 105$ K it undergoes a second order antiferrodistorsive cubic-tetragonal O_h^1 to D_{4h}^{18} structural transition with condensation of the Γ_{25} mode [3, 4]. The dielectric permittivity strongly rises on cooling, the lowest transverse optical (TO) phonon mode softens (incipient ferroelectricity) and the STO paraelectric central inversion phase nearly loses stability. However, in the low-temperature region of dominating quantum statistics, the ferroelectric instability is inhibited and the paraelectric phase is maintained due to quantum mechanical effects (quantum paraelectricity) [5–7].

By controlling the balance between the dipole–dipole interaction and the quantum fluctuation through doping [8], external field [3], pressure [9] or isotope exchange (^{16}O with ^{18}O) [10], this material shows the so-called quantum ferroelectricity.

There is long debate about the mechanisms of the phase transition in STO18 starting from the displacive type caused by the condensation of the ferroelectric E_u soft mode [11–13] ending with order–disorder component in addition to the displacive soft mode one [14, 15].

The structure of STO has been studied by different experiments: x-ray diffraction [2, 17], neutron diffraction [16] and x-ray absorption spectroscopy [18–26].

The aim of this work is the study of STO16 and STO18 with x-ray absorption spectroscopy, giving insight into local structure of Ti atom. At the same time, we have used optical second harmonic generation to indicate the presence on non-centrosymmetric phase in STO18.

2. Experimental and data analysis

In our study we used two samples: standard $SrTi^{16}O_3$ (powder and monocrystal) with ^{16}O (STO16) and $SrTi^{18}O_3$ where 96% of oxygen atoms were substituted by ^{18}O isotope (STO18). STO18 sample preparation procedure is described in [11].

The Ti K-edge x-ray absorption spectra were measured in fluorescence and transmission mode at the ESRF

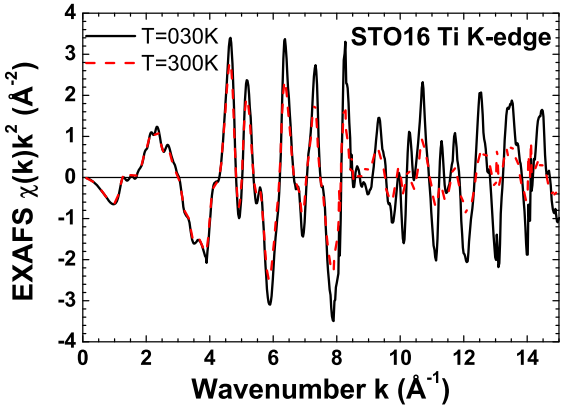

Figure 1. Ti K-edge EXAFS spectra $\chi(k)k^2$ for $SrTiO_3$ at two temperatures.

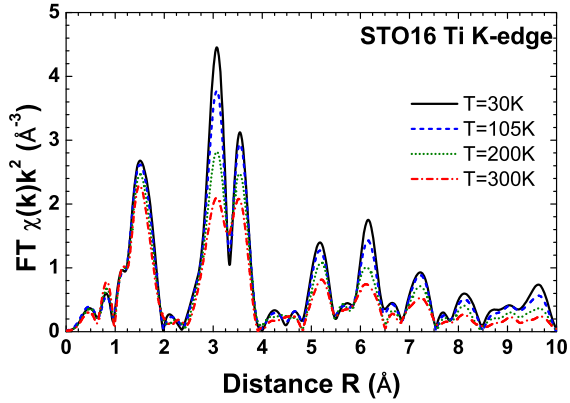

Figure 2. Fourier transform of the EXAFS spectra at several temperatures.

bending-magnet beamline BM23 and in transmission mode at the HASYLAB/DESY A1 bending-magnet beamline in the temperature range from 10 to 300 K.

The x-ray radiation was monochromatized by a 40% detuned Si(111) double-crystal monochromator, and the beam intensity was measured using two ionization chambers filled with argon and krypton gases and a Si drift detector for fluorescence mode. The Oxford Instruments liquid helium flow cryostat was used to maintain the required sample temperature. To achieve the best sample homogeneity and thickness at the Ti K-edge, necessary for transmission mode experiments, the proper amount of the STO powder was deposited on polytetraflouroethylene Millipore membranes from suspensions in methyl alcohol.

The extended x-ray absorption fine structure (EXAFS) oscillations $\chi(k)$ and x-ray absorption near edge structure (XANES) data were extracted and analyzed following the conventional procedure [27, 28] using the EDA software package [29]. Theoretical EXAFS signal (i.e. backscattering amplitude and phase-shifts functions) were calculated using FEFF8 code [30].

Optical second harmonic generation signal was excited by a wavelength-tunable pulsed solid state laser (pulse duration 30 ps) from Ekspla (PG401/SH pumped by the third harmonics of Nd:YAG laser). Excitation wavelength was 1064 nm. SH was measured by spectrograph/monochromator from BRUKER Optics (250is/sm) and detected by a streak camera from HAMAMATSU (C4334-01). The samples was mounted on the cold finger closed cycle cryostat (ARS-4HW, M/N DE-202E). The temperature of the samples varied from 15 K to RT and was controlled by LAKESHORE 325 temperature controller at precision of 1 K.

2.1. Extended x-ray absorption fine structure data

The extracted STO16 EXAFS spectra are shown in figure 1. The corresponding Fourier transforms of the EXAFS are shown in figure 2. One can notice that the peak corresponding to the first coordination shell (Ti–O_1) is less dependent on the temperature than the peaks corresponding to the second shell (Ti–Sr_2) and third shell (Ti–Ti_3) which have much stronger amplitude damping with temperature. This is an indication that the TiO_6 octahedra are relatively rigid

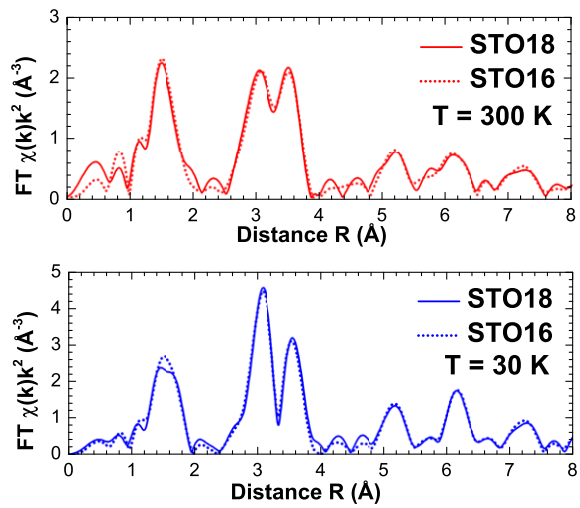

Figure 3. Comparison of the EXAFS spectra Fourier transform at different temperatures for STO16 and STO18.

compared, for example, with the Sr sublattice. The first coordination shell signal contains only the single scattering contribution. The peaks from the second (Ti–Sr_2) and the third (Ti–Ti_3) coordination shells, which are located between 2.5 and 4 Å are very close and cannot be separated; moreover they contain multiple scattering contributions from different Ti–O–O chains within octahedra.

As one can see from figure 3, spectra of STO18 and STO16 look very similar. This is expected because the difference in the structure between STO18 and STO16 is very small [10].

Conventional analysis [28] of the first coordination sphere of STO16 gives us values of the mean square relative displacement of the first coordination shell of Ti ($MSRD_{Ti-O_1}$) and the corresponding bond distance R_{Ti-O_1}. Amplitude factor has been kept constant (equal to the lowest temperature value), because the coordination number of Ti is assumed to be fixed. This has allowed us to avoid the well known correlation between MSRD and amplitude factor. In this paper, we concentrate on the behavior of the MSRD values seen in the figure 4, which contain a dynamic part, due to thermal oscillations, and a static one, originating from the differences of the distances Ti–O_1 within the first coordination shell (static disorder).

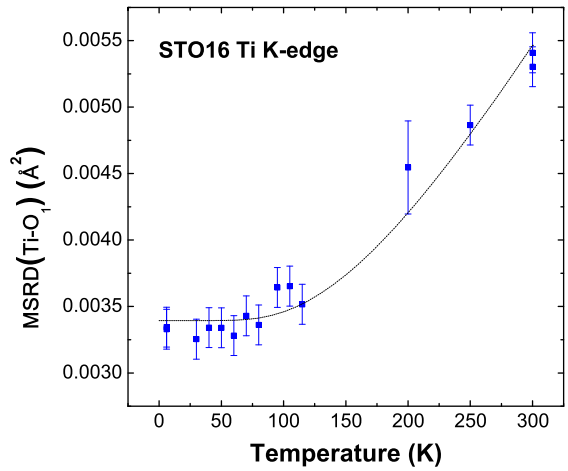

Figure 4. MSRD for Ti–O_1 bond for STO16. Line corresponds to the Einstein model.

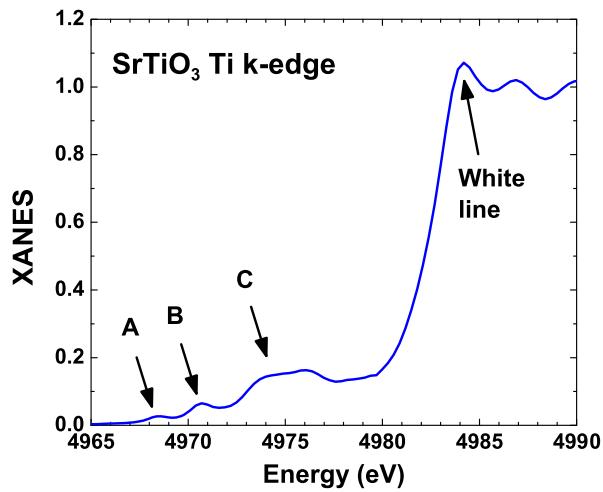

Figure 5. Ti K-edge XANES spectra for $SrTiO_3$ at $T = 10$ K. All three pre-peaks are labeled with A, B and C.

The temperature dependence of the $MSRD_{Ti-O_1}$ for STO16 within the experimental and procedural errors can be well approximated with the Einstein model [31], which is an indication that there are no significant local structure changes in the whole temperature range.

2.2. X-ray absorption near edge structure (XANES) data

Ti K-edge XANES spectrum in perovskites is very informative about off-center position of Ti atom [32, 33] due to the characteristic peaks in the pre-edge region (pre-peaks) shown in figure 5. In STO this region consists of three pre-peaks noted as 'A', 'B' and 'C'.

The first very small pre-peak ('A') comes from quadrupolar transition of Ti 1s electrons to Ti 3d-originated orbitals with t_{2g} symmetry.

The second pre-peak ('B') originates from transitions of Ti 1s electron to the p–d hybrid orbitals (e_g symmetry) originating from the titanium 3d orbital mixing with the oxygen 2p orbitals due to the Ti displacement from the center of the octahedra (violation of the inversion symmetry). According to Vedrinskii *et al* [33] the intensity of the pre-peak 'B' $\langle I_B \rangle$ is proportional to the squared displacement of the Ti

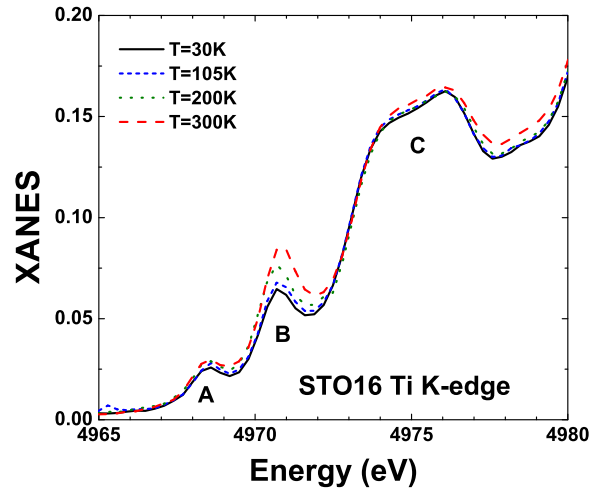

Figure 6. Temperature dependence of the STO16 Ti K-edge XANES spectra pre-peaks.

atoms from the centers of the oxygen octahedra $\langle \Delta r^2 \rangle$:

$$\langle I_B \rangle = K \frac{\langle \Delta r^2 \rangle}{3c^{5.5}}, \quad (1)$$

where c is lattice constant and K is a coefficient. Due to this relationship, the pre-peak 'B' is a very sensitive tool for probing the size of the Ti off-center positions. That is proved for $SrTiO_3$ by work of Cabaret *et al* [25], where the theoretical Ti K-edge XANES pre-edge structure was modeled using full-potential *ab initio* DFT calculations for various off-site Ti positions. Because of the small timescale of the x-ray absorption process (about 10^{-15} s) such signal is expected even in the case of the precisely symmetric TiO_6 octahedra, because of the thermal atomic oscillations. Thus, the amplitude of the pre-peak 'B' is modified as the dynamic part of MSRD (contribution of the thermal or quantum oscillations) but may contain some static part (displacement of the mean position of the Ti atom).

The third pre-peak ('C') is the largest and broadest. It comes from the dipole allowed transition from the 1s level of the absorbing Ti atom to the orbitals originated from the neighboring atoms.

As one can see from the temperature dependence of the XANES spectra (figure 6), the pre-peak 'B' has the more significant temperature dependence.

In order to compare data from the different samples of STO16 and STO18 at different temperatures at first we normalized XANES amplitudes to the amplitude of the white line, which is set to the equal value for all XANES measurements, and only then we calculated intensity of the pre-peak 'B'.

According to equation (1) the $\langle I_B \rangle$ should be proportional to the $MSRD_{Ti-O_1}$. Data shown in figure 7 confirm this suggestion and give us confidence about our data and methodology. This linear correlation helps us a lot, because it allows us to use the $\langle I_B \rangle$ signal, instead of MSRD. So in our further analysis we will concentrate on the studies of the behavior of the pre-peak 'B' intensity in STO18 compared with the STO16. As documented in figure 8, it is not a surprise that the temperature dependence of the pre-peak 'B'

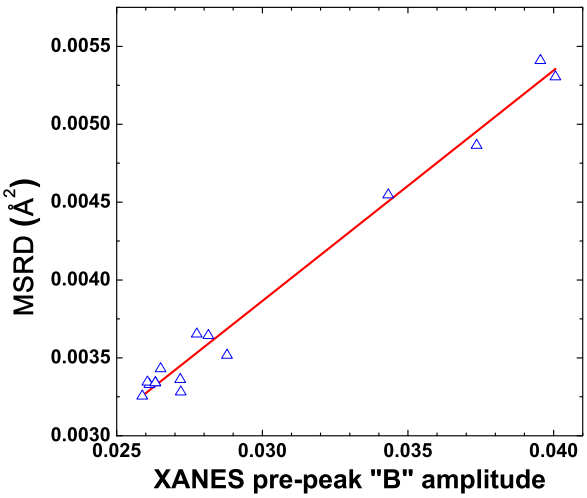

Figure 7. Correlation between Ti K-edge XANES pre-peak 'B' intensity and MSRD obtained from EXAFS for Ti first coordination shell in STO16.

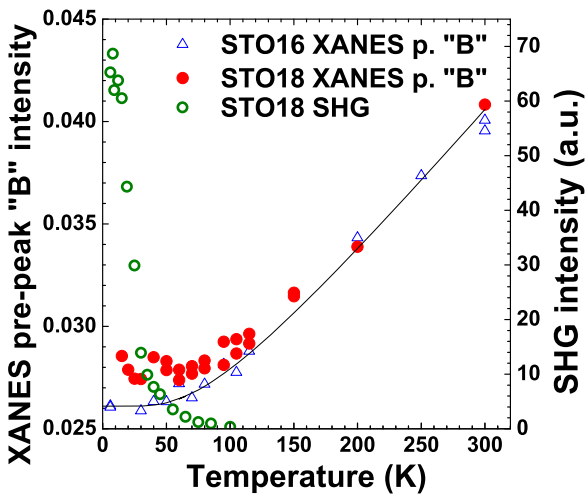

Figure 8. Temperature dependence of the XANES pre-peak 'B' for STO18 (red solid dots) compared with that of STO16 (blue triangles) and optical second harmonic generation signal from STO18 (green circles).

for STO16 follows the Einstein model in the same way as MSRD does. However, STO18 has a noticeable deviation in the low temperature region: STO18 has higher intensity of the pre-peak 'B' than STO16: the corresponding MSRD of Ti–O_1 bonds can be caused by larger movements of Ti atoms from the central position or/and by additional static off-center shifts compared with STO16.

By comparing XANES with the optical second harmonic signal, which is an excellent indicator of the non-centrosymmetric ferroelectric phase, one can see that these deviations strongly correlate. At the same time, in the low temperature region, we do not expect an increase of the Ti–O bonds vibration amplitude: with the increase of the oxygen mass the oscillation amplitudes should decrease. This leads us to the conclusion that there is an off-center position of the Ti atoms in the TiO_6 octahedra which is increasing when the temperature is decreasing. This phenomenon starts at least at 100 K, which is far above the suggested ferroelectric phase transition temperature $T_c = 25$ K. This correlates also with the optical second harmonic signal which also drops sharply at T_c, but to a non-zero value, because it slowly decreases until vanishes only at about 100 K.

This is a clear indication that the ferroelectric phase transition in the STO18 is not of a pure order–disorder type, because in this case the local off-center displacement of Ti atom should not change, and the MSRD should follow Einstein model and be flat in the low temperature region.

3. Conclusions

By comparing XANES of STO16 and STO18 we have identified the isotopic effect in STO18 which produces at $T <$ 100 K a strong deviation of mean square relative displacement of Ti–O_1 bonds from the Einstein model. The corresponding amplitude of the XANES pre-peak 'B' increases when temperature decreases. As in this temperature region it is unlikely that the atom oscillation amplitude increases, this is an indication of increasing off-center position of the Ti atom in the TiO_6 octahedra. This hypothesis is supported by the optical second harmonic signal which also after sharp decrease at the ferroelectric phase transition temperature slowly decreases, having non-zero value even at 100 K.

Acknowledgments

This work has been supported by the Latvian Science Council grant no. 402/2012, project CZ CZ.1.5/2.100/03.0058 of the MSMT CR, P108/12/1941 of the GACR, State via grant no. 8516 from MES of Russia, PP RAS 'Quantum mesoscopic and disordered systems' and European Social Fund within the project 'Support for Doctoral Studies at University of Latvia'. The authors thank Dr Olivier Mathon from ESRF and Dr Edmund Welter from DESY for assistance during the beamtimes.

References

[1] Lines M E and Glass A M 1977 *Principles and Applications of Ferroelectrics and Related Materials* (Oxford: Clarendon) p 680
[2] Lytle F W 1964 *J. Appl. Phys.* **35** 2212
[3] Fleury P A, Scott J F and Worlock J M 1968 *Phys. Rev. Lett.* **21** 16
[4] Shirane G and Yamada Y 1969 *Phys. Rev.* **177** 858
[5] Muller K A and Burkard H 1979 *Phys. Rev.* B **19** 3593
[6] Vaks V G 1973 *Introduction to Microscopical Theory of Ferroelectrics* (Moscow: Nauka) p 327 (in Russian)
[7] Kvyatkovskii O E 2001 *Phys. Sol. State* **43** 1401
[8] Bednorz J G and Müller K A 1984 *Phys. Rev. Lett.* **52** 2289
[9] Uwe H and Sakudo T 1976 *Phys. Rev.* B **13** 271
[10] Itoh M *et al* 1999 *Phys. Rev. Lett.* **82** 3540
[11] Taniguchi H, Itoh M and Yagi T 2007 *Phys. Rev. Lett.* **99** 017602
[12] Hasebe H, Tsujimi Y, Wang R, Itoh M and Yagi T 2003 *Phys. Rev.* B **68** 014109
[13] Takesada M, Itoh M and Yagi T 2006 *Phys. Rev. Lett.* **96** 227602
[14] Blinc R, Zalar B, Laguta V V and Itoh M 2005 *Phys. Rev. Lett.* **94** 147601
[15] Shigenari T, Abe K, Takemoto T, Sanaka O, Akaike T, Sakai Y, Wang R and Itoh M 2006 *Phys. Rev.* B **74** 174121

[16] Heidemann A and Wettengel H 1973 *Z. Phys.* **258** 429
[17] Schmidbauer M, Kwasniewski A and Schwarzkopf J 2012 *Acta Crystallogr.* B **68** 8
[18] Fischer M, Lahmar A, Maglione M, San Miguel A, Itie J P and Polian A 1994 *Phys. Rev.* B **49** 12451
[19] Ravel B and Stern E A 1995 *Physica* B **208/209** 316
[20] Kamishima O, Nishihata Y, Maeda H, Ishii T, Sawada A and Terauchi H 1995 *Physica* B **208/209** 303
[21] Nozawa S, Iwazumi T and Osawa H 2005 *Phys. Rev* B **72** 121101
[22] Andreasson B P, Janousch M, Staub U, Meijer G I and Delley B 2007 *Mater. Sci. Eng.* B **144** 60
[23] Hashimoto T, Yoshiasa A, Okube M, Okudera H and Nakatsuka A 2007 *AIP Conf. Proc.* **882** 428
[24] Vračar M, Kuzmin A, Merkle R, Purans J, Kotomin E A, Maier J and Mathon O 2007 *Phys. Rev.* B **76** 174107
[25] Cabaret D, Couzinet B, Flank A M, Itié J P, Lagarde P and Polian A 2007 *AIP Conf. Proc.* **882** 120
[26] Levin I, Krayzman V, Woicik J C, Tkach A and Vilarinho P M 2010 *Appl. Phys. Lett.* **96** 052904
[27] Rehr J J and Albers R C 2000 *Rev. Mod. Phys.* **72** 621
[28] Aksenov V L, Kovalchuk M V, Kuzmin A, Purans J and Tyutyunnikov S I 2006 *Crystallogr. Rep.* **51** 908
[29] Kuzmin A 1995 *Physica* B **208-209** 175
[30] Ankudinov A L, Ravel B, Rehr J J and Conradson S D 1998 *Phys. Rev.* B **58** 7565
[31] Gao H X, Penga L-M and Zuo J M 1999 *Acta Crystallogr.* A **55** 1014
[32] Ravel B, Stern E A, Vedrinskii R I and Kraizman V 1998 *Ferroelectric* **206** 407–30
[33] Vedrinskii R V, Kraizman V L, Novakovich A A, Demekhin Ph V and Urazhdin S V 1998 *J. Phys.: Condens. Matter* **10** 9561